Journal of Nano- and Electronic Physics
Vol. **17** No 2, 02015(7pp) (2025)

Журнал нано- та електронної фізики
Том **17** № 2, 02015(7cc) (2025)

REGULAR ARTICLE

Reflection of Bilateral Porous Silicon with Macropores or Nanowires

V.F. Onyshchenko *, L.A. Karachevtseva

V.Ye. Lashkaryov Institute of Semiconductor Physics of National Academy of Sciences of Ukraine, 03028 Kyiv, Ukraine

(Received 01 February 2025; revised manuscript received 23 April 2025; published online 28 April 2025)

The reflection of bilateral porous silicon with macropores or nanowires is calculated according to analytically derived formulas. The formulas take into account the multiple reflections of light at all angles in each porous layer and monocrystalline substrate. Layers of porous silicon are considered as effective media with Lambertian surfaces. The reflection of bilateral macroporous silicon depends on the volume fraction of the pores of the frontal porous layer. The thickness of the frontal layer of macroporous silicon affects the reflection spectrum of bilateral macroporous silicon when the volume fraction of pores is greater than 0.2. The influence of the thickness of the frontal layer of macroporous silicon on the reflectance spectrum of bilateral macroporous silicon increases as the volume fraction of pores increases. The volume fraction of pores of the back porous layer affects the reflection spectrum of bilateral macroporous silicon at wavelengths of light greater than 1.05 μm. The volume fraction of pores of the back layer of macroporous silicon affects the reflection spectrum of bilateral macroporous silicon at wavelengths of light greater than 1.05 μm.

Keywords: Reflection, Bilateral porous silicon, Macroporous silicon, Nanowires.

DOI: 10.21272/jnep.17(2).02015 PACS number: 78.20. – e

1. INTRODUCTION

A single crystal of silicon structured by pores, nanowires and pyramids is a single crystal with a porous layer. The porous layer is an effective medium when the wavelength of light exceeds the dimensions of the structural elements. The structured surface improves light absorption. The solar element captures the light. Capture occurs due to multiple reflections of light in the middle of the solar cell between its surfaces. The effect of light trapping by a solar cell is modelled by ray tracing. The reflectivity of silicon thin film on V-shaped glass approaches the reflectivity of silicon structured by pyramids. The simulation results are verified by experimental data [1]. The optical properties of multicrystalline silicon solar cells are modelled using the spherical cap model. The spectral dependence of the reflection coefficient and the generation of charge carriers of the cell is calculated taking into account the light trapping by the solar cell [2]. A theoretical model of the reflection of arrays of silicon nanowires and macroporous silicon is presented. The model considers porous silicon as an effective medium and takes into account the multiple reflection of light from the sample surfaces [3]. Light trapping by a solar cell structured by randomly located real pyramids is compared with a similar structure but with a pyramid base angle equal to 54.7° (ideal pyramids) and Lambertian scatterers. Calculations were performed using ray tracing simulation. The angular distribution of light intensity is calculated for each reflection from the frontal and rear surfaces [4, 5]. A new indicator of light trapping efficiency of nanostructured solar cells is proposed. The indicator of light trapping efficiency evaluates the nanostructure, so it does not depend on the choice of material [6]. The optical and electronic properties of black silicon are studied. Nanostructured monocrystal-line black silicon is passivated by depositing an atomic layer of aluminum oxide on the structured surface. The surface recombination velocity of passivated black silicon was equal to 0.13 m/s. The lifetime of minor charge carriers in black silicon is milliseconds [7]. The kinetics of charge carriers and photoconductivity in bilateral macroporous silicon was calculated by the finite difference method. Stationary photoconductivity was excited by light with a wavelength of 0.95 μm and 1.05 μm. On a semilogarithmic scale, the decline in photoconductivity changes its slope when the pore depth of one of the macroporous layers exceeds 250 μm [8, 9]. An optical analysis of a solar cell with periodically located pyramids was carried out. The pyramids are located on the frontal surface. The reflection and absorption coefficient of a solar cell with periodically arranged pyramids is studied depending on the size of the pyramids. The reflection coefficient from the back side of the solar cell does not depend on the size of the pyramids, if their size is more than 0.6 μm [10]. The distribution of reflection from the surface of silicon solar cells structured by pyramids is analyzed. The base angle of the texture affects the reflectivity of the solar

* Correspondence e-mail: onyshchenkovf@isp.kiev.ua

Cite this article as: V.F. Onyshchenko et al., *J. Nano- Electron. Phys.* 17 No 2, 02015 (2025) https://doi.org/10.21272/jnep.17(2).02015

cell, light capture, photo generation and recombination on the surface [11]. The photoconductivity and concentration of charge carriers in bilateral macroporous silicon were calculated. The photoconductivity of bilateral macroporous silicon decreases if the pore depth increases and the life-time decreases [12]. An experimental study of the optical properties and the etching process of a silicon wafer confirm the influence of the surface structure on light capture. Scanning electron microscopy and atomic force microscopy were used to study the effect of surface structure [13]. Structures with a non-homogeneous refractive index are theoretically studied. The light trapping structure is placed on top of the solar cell [14]. The reflectance of two-layer porous silicon is lower than that of single-crystal silicon and single-layer porous silicon, due to the optimization of the pore volume fraction. The optimization is carried out by the gradient descent method [15].

2. REFLECTION OF BILATERAL MACROPOROUS SILICON AND NANOWIRES

Fig. 1 shows a diagram of bilateral macroporous silicon with a thickness of h. Light falls on a macroporous layer with a thickness of h_1, perpendicular to its surface. This macroporous layer is the frontal macroporous layer. The back macroporous layer has a thickness of h_2, it is located on the other side of the monocrystalline substrate with a thickness of $hm = h - h_1 - h_2$. A structure with silicon columns or nanowires, which are located on two sides of a single crystal, has a similar scheme. Layers of macro-porous silicon are considered effective media. Their structured surfaces scatter light. Let's distinguish four surfaces: the frontal surface (light falls on this surface), the second surface, the third surface and the back surface. The second and third surfaces are the surfaces of the monocrystalline substrate. All sur-faces scatter light according to Lambert's law, so let's call them Lambert surfaces.

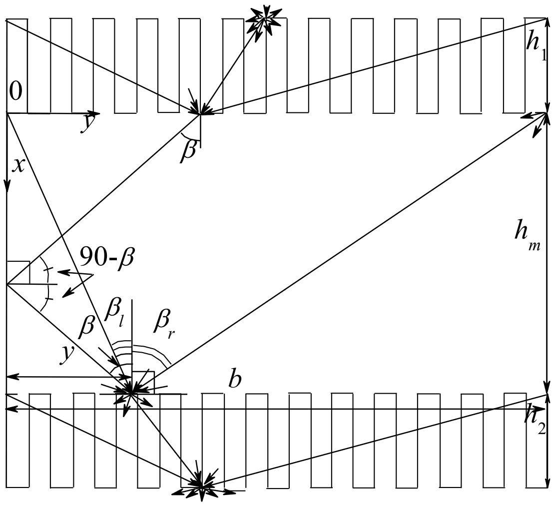

Fig. 1 – Scheme of bilateral macroporous silicon with reflection of rays from its surfaces

First, consider the reflection of the monocrystalline substrate. The reflection of macroporous layers is similar, because they are effective media. Let's choose a coordinate system. The x axis is directed perpendicular to the frontal surface (see Fig. 1). The origin of the coordinates is at the intersection of the left side and the second surface (in the two-dimensional case, these are segments), the y axis is directed along the plate, as shown in Fig. 1. The length of the plate is b. Let the light with intensity I_0 fall on the second surface, which is the surface of the monocrystalline substrate. It is a Lambertian surface. Each point of the Lambertian surface scatters the reflected light according to the cosine law. The intensity of light reflected by the Lambertian (second) surface at an angle β is written as follows: $I_0R_s{}^*\cos(\beta)$, where the angle β varies from 0 to $\pi/2$, R_{s2^*} is the reflection coefficient from the boundary of the frontal layer of macroporous silicon with a monocrystalline substrate (second surface). The intensity of the light that passed through the second surface and was scattered at an angle β: $I_0(1 - R_{s^*})\cos(\beta)$. The light intensity on the third surface is equal to $I = I_0 \sin(\beta)\cos(\beta)$. Each point of the second surface emits light into the middle of the monocrystalline substrate with an intensity that depends on the radiation angle according to the cosine law. Light passes through the monocrystalline substrate, is absorbed and falls on a third surface. It can also be reflected from the side surface according to Snell's law and Fresnel's formula, and then it al-ready falls on the third surface, as shown in Fig. 1. Light is completely reflected if it falls on the side sur-face at angles greater than the critical angle of total internal reflection. To describe the above, let's choose a point with the y coordinate on the third surface. The intensity of light that came from all angles and falls on a point with the y coordinate will be written as:

$$I_0(1-R_{s2*})\int \sin(\beta)\cos(\beta)\exp(-\frac{\alpha h_m}{\cos(\beta)})d\beta \qquad (1)$$

Eq. (1) has an exponent because silicon absorbs with an absorption coefficient α. Light propagating at an angle β will pass the optical path $h_m/\cos(\beta)$. The distance from the point with coordinate y to the left side surface is equal to y, and to the right-side sur-face is equal to $b - y$ (see Fig. 1). Select the angles $\beta_l(h_m, y)$ and $\beta_l(h_m, b - y)$. They limit the fall of light from the side surfaces to a point with the y coordinate. The left angle of incidence is $\beta_l(h_m, y) = \arctan(y/h_m)$. The right angle is similar to $\beta_l(h_m, b - y) = \arctan(b - y)/h_m)$. Fig. 1 shows the angle β. This angle is equal to the angle of incidence of light on the third surface, regardless of whether the light is reflected from the side surface or not. The next characteristic angle is the critical angle of total internal reflection β_c. The critical angle of total internal reflection for silicon is equal to: $\beta_c = \mathrm{acrsin}(1/n_{Si})$. Light falls on the side surface at angles greater than the critical angle of total internal reflection measured from the perpendicular to the side surface, when it falls at angles less than 90 degrees minus the critical angle of total internal reflection measured from the perpendicular to the second surface. This is due to the fact that the angles of incidence on the side surface and on the third surface differ by 90 degrees. Consider the case when the angle equal to 90 degrees minus the critical angle of total internal reflection calculated from the perpendicular to the second surface is greater than the angle limiting the side surface $\pi/2 - \beta_c > \beta_l(h_m, y)$. Light is completely reflected from the side surface and falls on the third surface if it falls at angles greater than the angle limiting the side surface, but less than an angle equal to 90 degrees minus the critical angle of total internal reflection calculated from the perpendicular to the second surface. That is, the limits of integration are from zero to $\pi/2 - \beta_c$. In the case when $\pi/2 - \beta_c < \beta_l(h_m, y)$ the entire lateral surface reflects and refracts light, so the limits of integration are from zero to $\beta_l(h_m, y)$. Based on the above, the limits of integration will be written as:

$$\beta(h_m, y) = \begin{cases} \arctan\left(\dfrac{y}{h_m}\right), \text{ якщо } \arctan\left(\dfrac{y}{h_m}\right) < \dfrac{\pi}{2} - \arcsin\left(\dfrac{1}{n_{Si}}\right) \\ \dfrac{\pi}{2} - \arcsin\left(\dfrac{1}{n_{Si}}\right), \text{ в інших випадках} \end{cases} \quad (2)$$

The limits of integration for the right-hand side are similar to those for the left-hand side. They will be written as: $\beta(h_m, b - y)$. Eq. (1) will have the reflection coefficient under the integral for angles from $\beta(h_m, y)$ (or $\beta(h_m, b - y)$) to $\pi/2$. The distribution of light intensity on the third surface, after the passage of light from the second to the third surface, is written as:

$$\begin{aligned} I_{23}(h_m, y) = \frac{I_0}{2}(1 - R_{s2*}) \Bigg(& \int_0^{\beta(hm,y)} \sin(\beta)\cos(\beta)\exp\left(-\frac{\alpha h_m}{\cos(\beta)}\right)d\beta + \\ & + \int_0^{\beta(hm,b-y)} \sin(\beta)\cos(\beta)\exp\left(-\frac{\alpha h_m}{\cos(\beta)}\right)d\beta + \\ & + \int_{\beta(hm,y)}^{\frac{\pi}{2}} R(\beta)\sin(\beta)\cos(\beta)\exp\left(-\frac{\alpha h_m}{\cos(\beta)}\right)d\beta + \\ & + \int_{\beta(hm,b-y)}^{\frac{\pi}{2}} R(\beta)\sin(\beta)\cos(\beta)\exp\left(-\frac{\alpha h_m}{\cos(\beta)}\right)d\beta \Bigg) \end{aligned} \quad (3)$$

The first two integrals calculate the intensity of light falling from the second surface to the third surface without loss of intensity on the side surfaces. The third and fourth integrals calculate the intensity of light falling from the second surface to the third surface after reflecting off the side surfaces with losses. A monocrystalline substrate has two Lambert surfaces. Light falling from the second to the third surface and vice versa from the third to the second surface is equally scattered and absorbed, because the monocrystalline substrate is symmetrical with respect to the plane passing through the middle of the monocrystalline substrate. The radiation of each point of the light intensity distribution on the third surface falls on the second surface in accordance with the distribution given by Eq. (3) with the limit of integration (2). That is, the Eq. (3) with the limit of integration (2) is a transformation. This transformation trans-forms the distribution of light intensity on the second surface into a distribution on the third plane, and then again on the second surface, and so on ad infinitum. The normalized distribution of light intensity on the surface, after the passage of light from one surface to another (normalized distribution of light intensity) will be written as:

$$\begin{aligned} I_b(h_m, y) = \frac{1}{2} \Bigg(& \int_0^{\beta l(y)} \sin(\beta)\cos(\beta)\exp\left(-\frac{\alpha h_m}{\cos(\beta)}\right)d\beta + \\ & + \int_0^{\beta r(y)} \sin(\beta)\cos(\beta)\exp\left(-\frac{\alpha h_m}{\cos(\beta)}\right)d\beta + \\ & + \int_{\beta l(y)}^{\frac{\pi}{2}} R(\beta)\sin(\beta)\cos(\beta)\exp\left(-\frac{\alpha h_m}{\cos(\beta)}\right)d\beta + \\ & + \int_{\beta r(y)}^{\frac{\pi}{2}} R(\beta)\sin(\beta)\cos(\beta)\exp\left(-\frac{\alpha h_m}{\cos(\beta)}\right)d\beta \Bigg) \end{aligned} \quad (4)$$

The average value of the normalized distribution of light intensity on the surface after the passage of light from one surface to another is written as:

$$\begin{aligned} I_b(h_m) = \frac{1}{2b} \int_0^{\beta} \Bigg(& \Big(\int_0^{\beta l(y)} \sin(\beta)\cos(\beta)\exp\left(-\frac{\alpha h_m}{\cos(\beta)}\right)d\beta + \\ & + \int_0^{\beta r(y)} \sin(\beta)\cos(\beta)\exp\left(-\frac{\alpha h_m}{\cos(\beta)}\right)d\beta + \\ & + \int_{\beta l(y)}^{\frac{\pi}{2}} R^{kr(\beta)}\sin(\beta)\cos(\beta)\exp\left(-\frac{\alpha h_m}{\cos(\beta)}\right)d\beta + \\ & + \int_{\beta r(y)}^{\frac{\pi}{2}} R^{kr(\beta)}\sin(\beta)\cos(\beta)\exp\left(-\frac{\alpha h_m}{\cos(\beta)}\right)d\beta\Big) \Bigg) dy \end{aligned} \quad (5)$$

The reflection and transmittance coefficients of the monocrystalline substrate are calculated using the normalized distribution of light intensity (4) and its average value (5). The reflection coefficient of a monocrystalline substrate consists of the sum whose terms are formed due to the fact that light is reflected inside the monocrystalline substrate and then exits through the second surface. Each point of the second surface will scatter light according to the law of cosines if it exits the monocrystalline substrate through the second surface. The first term of the distribution of the reflection coefficient of a monocrystalline substrate:

$$\begin{aligned} R_{m1}(h_m, y, \gamma) = (1 - R_{s2*})(1 - R_{s2}) \times \\ \times R_{s3} I_b(h_m) I_b(h_m, y)\cos(\gamma) \end{aligned} \quad (6)$$

where γ is the angle of light scattering by the Lambertian surface, R_{s2}, R_{s3} are the reflection coefficient from the boundary of the monocrystalline substrate with the frontal and back layers of macroporous silicon, respectively. Eq. (6) contains the product of transmission coefficients through the second surface $(1 - R_{s*})(1 - R_s)$ because the light passes through the second surface twice. It passes through the surface from different sides. The reflection coefficients from the boundary of a layer of macroporous silicon with a monocrystalline substrate and the boundary of a monocrystalline substrate with a layer of macroporous silicon differ when light is incident at an angle to the surface. The macroporous silicon layer has an effective refractive index. The product is multiplied by the normalized distribution of light intensity (4) because the light passes from the third surface to the second surface. The light intensity on the third surface is shown by the product of the reflection coefficient from the boundary of the monocrystalline substrate with a frontal macroporous layer by the average value of the normalized light intensity distribution (5). We took the average value of the normalized distribution of light intensity on the third surface to simplify the problem. It becomes clear that when the light will be reflected from the surface next time, then it is necessary to multiply by the product of the reflection coefficient by the average value of the normalized distribution of light intensity (5). The light exits a second time through the second surface, reflecting off the surfaces three times. It is reflected twice from the third surface and once from the second surface. The second product of the re-flection coefficient from the monocrystalline substrate will differ from the first by the product of the reflection coefficients from the second and third surfaces by the average value of the normalized distribution of light intensity (5). The second term of the distribution of the light reflection coefficient from the monocrystalline substrate will be written as:

$$R_{m2}(h_m, y, \gamma) = (1 - R_{s*})(1 - R_{s2}) \times \times R_{s2} R_{s3}^2 I_b^3(h_m) I_b(h_m, y)\cos(\gamma) \quad (7)$$

Eq. (7) contains the product of the reflection coefficients from the second surface and the third surface squared by the average value of the normalized light intensity distribution (5) in the third power, because light is reflected three times. Light is reflected from the third surface, from the second surface, again from the third surface and exits through the second surface. The normalized intensity distribution (4) must be multiplied by the product of the reflection coefficient from the second surface to the power of $n - 1$ by the reflection coefficient from the third surface to the power of n by the average value of the normalized in-tensity distribution (5) to the power of $2n - 1$ and by the product of the transmission coefficients through the second surface from different sides $(1 - R_{s2*})(1 - R_{s3})$, when the light passes through the second surface n times. Each passage of light through the second surface adds one more term to the sum of which the resulting distribution of the light reflection coefficient from the monocrystalline substrate will consist of. The distribution of the light reflection coefficient from the mono-crystalline substrate will be written in the form:

$$R_m(h_m, y, \gamma) = \cos(\gamma)\left(R_{s2*} + (1 - R_{s2*})(1 - R_{s2}) \times \times I_b(h_m, y)\sum_{n=0}^{\infty}\left(R_{s2}^{n-1} R_{s3}^n I_b^{2n-1}(h_m)\right)\right) \quad (8)$$

The sum in Eq. (8) goes to the fraction, so the distribution of the light reflection coefficient from the monocrystalline substrate will be written as:

$$R_m(h_m, y, \gamma) = \cos(\gamma) \times \times\left(R_{s*} + \frac{(1 - R_{s*})(1 - R_s) R_{s3} I_b(h_m)}{1 - R_{s2} R_{s3} I_b^2(h_m)} I_b(h_m, y)\right) \quad (9)$$

The average reflection coefficient from a monocrystalline substrate:

$$R_m = \frac{1}{b}\int_0^b R_m(h_m, y, \gamma)dy = \left(R_{s*} + \frac{(1 - R_{s2*})(1 - R_{s2})}{1 - R_{s2} R_{s3} I_b^2(h_m)} \times \times \frac{R_{s3} I_b(h_m)}{b}\int_0^b I_b(h_m, y)dy\right)\int_0^{\pi/2}\cos(\gamma)d\gamma \quad (10)$$

or:

$$R_m = R_{s2*} + \frac{(1 - R_{s2*})(1 - R_{s2}) R_{s3} I_b^2(h_m)}{1 - R_{s2} R_{s3} I_b^2(h_m)} \quad (11)$$

Let's calculate the reflection coefficient from the bilateral macroporous silicon plate, which consists of three layers, two macroporous layers and a monocrystalline substrate. Macroporous layers are effective media for wavelengths larger than the pore structure, so we apply Eq. (11) for them. Consider the reflection from the second surface of the macroporous layer as the reflection from the second surface together with the monocrystalline substrate. Then we consider the reflection from the monocrystalline substrate and its third surface. The reflection from the third surface is equal to the reflection from the third surface together with the back macroporous layer. The reflection coefficient from two-sided macroporous silicon will be written as:

$$R_{bmSi} = R_{s1*} + \frac{(1 - R_{s1*})(1 - R_{s1}) R_{s23} I_{b1}^2(h_1)}{1 - R_{s1} R_{s23} I_{b1}^2(h_1)} \quad (12)$$

where:

$$R_{s23} = R_{s2*} + \frac{(1 - R_{s2*})(1 - R_{s2}) R_{s34} I_{b2}^2(h - h_1 - h_2)}{1 - R_{s2} R_{s34} I_{b2}^2(h - h_1 - h_2)} \quad (13)$$

where:

$$R_{34} = R_{s3*} + \frac{(1 - R_{s3*})(1 - R_{s3}) R_{s4} I_{b3}^2(h_2)}{1 - R_{s3} R_{s4} I_{b3}^2(h_2)} \quad (14)$$

3. RESULTS AND DISCUSSION

Fig. 2 shows the reflection spectrum of bilateral macroporous silicon with different volume fraction of pores. Arrays of nanowires placed on both sides of a monocrystalline substrate have a similar reflection spectrum. The thickness of bilateral macroporous silicon is 500 μm. The thickness of the frontal layer of macroporous silicon is 20 μm, the thickness of the back layer of macroporous silicon is 50 μm. The curve 1 on Fig. 2 is the reflection spectrum of single crystal silicon.

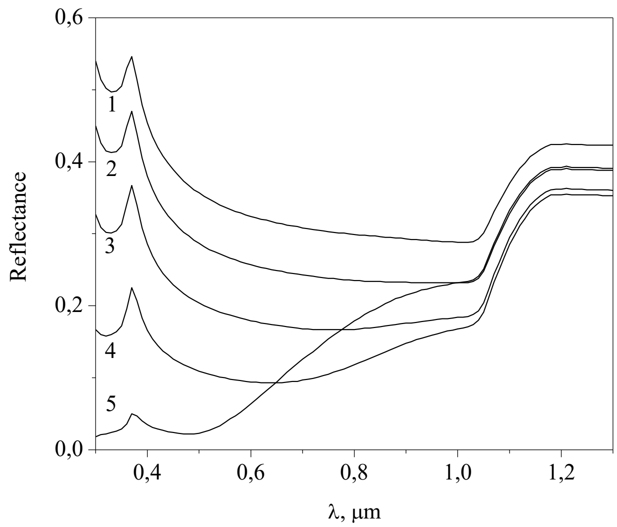

Fig. 2 – The reflection spectrum of bilateral macroporous silicon with pores or nanowires with a volume fraction of pores: 1–0; 2–0.1; 3–0.3; 4–0.5, 5–0.7. The thickness of the frontal macroporous silicon is 20 μm, the thickness of the rear macroporous silicon is 50 μm

The reflection spectrum of monocrystalline silicon contains the reflection of the surface of air - monocrystalline silicon, to which is added the reflection caused by the back surface at wavelengths of light greater than 1.05 μm. Light emerges from the frontal surface if it is not absorbed by the silicon. The reflection spectrum of bilateral macroporous silicon decreases with an increase in the volume fraction of pores. This is due to the reduction of the difference between the refractive indices of air and the frontal macroporous layer. The reflection from the second surface begins to appear on the reflection spectrum already at a volume fraction of pores of 0.3 (Fig. 2, curve 3). A small increase in the reflection of light with wavelengths greater than 0.8 μm is observed. When the volume fraction of pores is equal to 0.5 and 0.7, the difference between the refractive indices of the monocrystalline substrate and the frontal macroporous layer is large, therefore the reflection from the second plane is also large. The frontal macroporous layer with a thickness of 20 μm does not absorb waves larger than 0.5 μm (curve 5) and 0.7 μm (curve 4). The reflection from the third and back surfaces of the two-sided macroporous silicon increases due to absorption by the 500 μm thick macroporous silicon sample, but not significantly. At the same time, the difference between the refractive indices of the frontal macroporous layer and air is not great, so the reflection from the frontal surface of the bilateral macroporous silicon is a small 0.02 (see Fig. 2, curve 5). The reflection from the frontal surface of the bilateral macroporous silicon is hidden by reflection of the second surface.

Fig. 3 shows the reflection spectrum of bilateral macroporous silicon with pores or nanowires at different volume fractions of pores. The sample is illuminated from the other side. That is, the thickness of the frontal layer of macroporous silicon is 50 μm, and the thickness of the back layer of macroporous silicon is 20 μm.

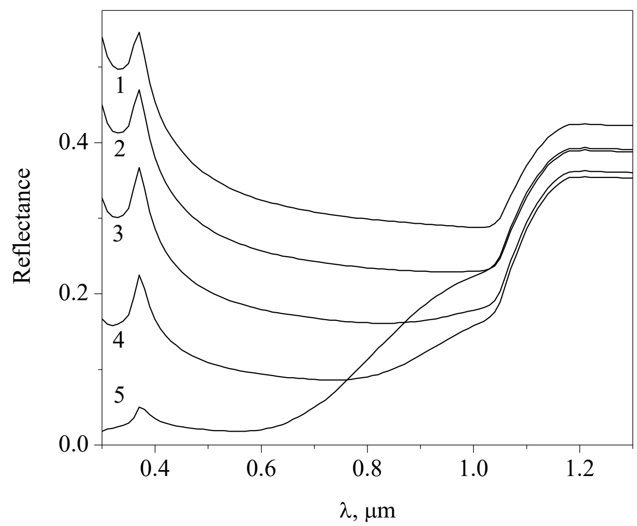

Fig. 3 – The reflection spectrum of bilateral macroporous silicon with pores or nanowires with a volume fraction of pores: 1–0; 2–0.1; 3–0.3; 4–0.5, 5–0.7. The thickness of the frontal macroporous silicon is 50 μm, the thickness of the rear macroporous silicon is 20 μm

There is a similarity between Fig. 2 and Fig. 3, but there are also differences. The frontal macroporous layer became thicker, and the back macroporous layer became thinner, so the reflection spectrum of the second surface shifted and decreased in intensity. The reflection spectrum of the second surface appears when the volume fraction of pores is greater than 0.3 (see Fig. 3, curve 3). The reflection spectra of double-sided macroporous silicon when illuminated from the side of the macroporous layer with a thickness of 20 μm and 50 μm are the same for wavelengths longer than 1 μm.

Fig. 4 shows the reflection spectrum of bilateral macroporous silicon with pores or nanowires with different volume fraction of pores and thickness of the frontal layer of macroporous silicon. The volume fraction of the back layer of macroporous silicon is 0.2, and its thickness is 50 μm. The reflection spectrum of bilateral macroporous silicon does not depend on the thickness of the frontal layer of macroporous silicon when the volume fraction of pores is less than 0.2 (see Fig. 4, curve 2). The dependence of the magnitude of the reflection spectrum of bilateral macroporous silicon on the thickness of the frontal layer of macroporous silicon increases when the volume fraction of pores increases (see Fig. 4). The reflection spectrum from the second surface is added to the reflection spectrum from the front surface. The magnitude of the reflection spectrum from the second surface is 0.02 when the volume fraction of pores is 0.4. The value of the reflection spectrum increases for wavelengths of light from 0.4 μm to 1.05 μm, when the thickness of the macroporous silicon layer decreases from 100 μm to 0.1 μm (see Fig. 4 curves 3–10). The magnitude of the reflection spectrum from the second surface is 0.1 when the volume fraction of pores is 0.7 (see Fig. 4, curves 7–10).

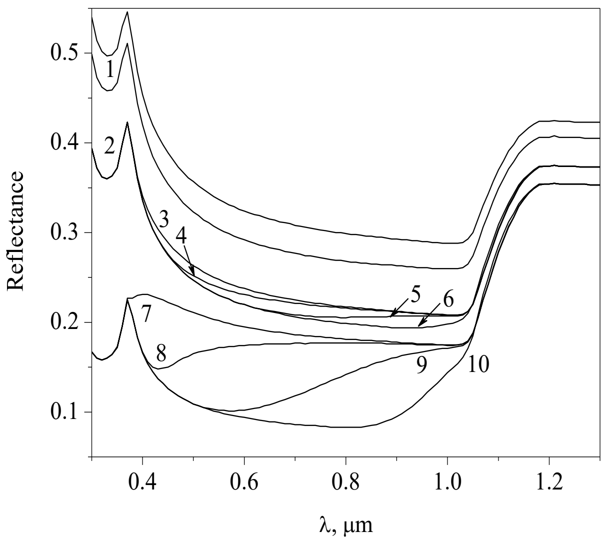

Fig. 4 – The reflection spectrum of bilateral macroporous silicon with pores or nanowires with the volume fraction of pores of the frontal layer of macroporous silicon: 1–0; 2–0.2; 3–6–0.4; 7–10–0.7 and its thickness, μm: 2, 3, 7–0.1; 2, 4, 8–1; 2, 5, 9–10; 2, 6, 10–100. The volume fraction of pores and the thickness of the back layer of macroporous silicon are 0.2 and 50 μm, respectively

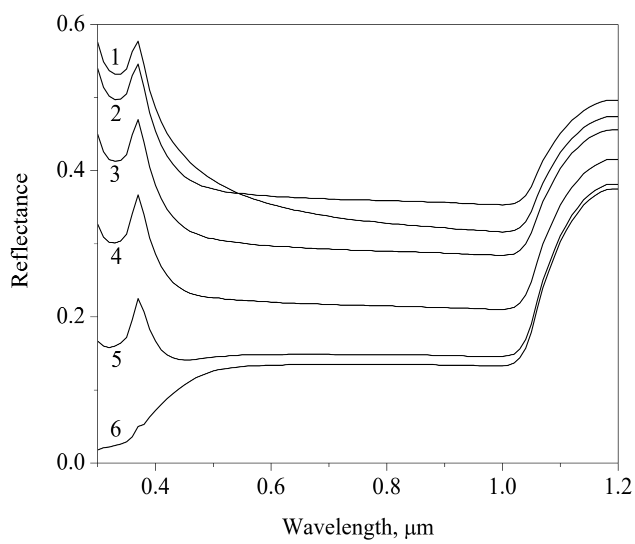

Fig. 5 – The reflection spectrum of bilateral macroporous silicon with pores or nanowires with the volume fraction of pores of the back layer of macroporous silicon: 1–0; 2–0.1; 3–0.3; 4–0.5, 5–0.7. The volume fraction of pores of the frontal layer of macroporous silicon is 0.6

Fig. 5 shows the reflection spectrum of bilateral macroporous silicon with pores or nanowires with different volume fraction of pores of the back layer of macroporous silicon. The volume fraction of pores of the frontal layer of macroporous silicon is 0.6, and its thickness is 20 μm. The thickness of the back layer of macroporous silicon is 50 μm. The volume fraction of the porous macroporous layer affects the reflection spectrum of bilateral macroporous silicon only at wave-lengths of light greater than 1.05 μm. Bilateral macroporous silicon absorbs light with wavelengths shorter than 1.05 μm. The reflection spectrum of bilateral macroporous silicon decreases in intensity when the volume fraction of the porous macroporous layer increases. Moreover, the decrease in the intensity of the reflection spectrum slows down. The intensity of the reflection spectra of bilateral macroporous silicon differs by only 0.01 when the volume fraction of the back macroporous layer is 0.5 and 0.7.

4. CONCLUSION

The magnitude of the reflectance spectrum of bilateral macroporous silicon decreases with an increase in the volume fraction of pores. This is due to the reduction of the difference between the refractive indices of air and the effective medium of the frontal macroporous layer. The effective absorption coefficient of the effective medium of the frontal macroporous layer decreases due to the decrease in the volume fraction of silicon. The reflection spectrum of bilateral macroporous silicon changes when the sample is illuminated from the opposite side, another layer of macroporous silicon, which has a different volume fraction of pores and thickness.

The reflection spectrum of bilateral macroporous silicon depends on the thickness of the frontal layer of macroporous silicon when the volume fraction of pores is greater than 0.2. The dependence of the magnitude of the reflection spectrum of bilateral macroporous silicon on the thickness of the frontal layer of macroporous silicon increases when the volume fraction of pores increases. The magnitude of the reflection spectrum from the second surface is 0.1 when the volume fraction of pores is 0.7.

The volume fraction of the back macroporous layer affects the reflection spectrum of bilateral macroporous silicon at wavelengths of light greater than 1.05 μm. Bilateral macroporous silicon with a thickness of 500 μm completely absorbs light with wavelengths shorter than 1.05 μm. The reflection spectrum of bilateral macroporous silicon decreases in intensity when the volume fraction of the back macroporous layer increases. Moreover, the decrease in the intensity of the reflection spectrum slows down due to the increase in reflection from the boundary of the frontal macroporous silicon with a monocrystalline substrate.

REFERENCES

1. T. Yagi, Y. Uraoka, T. Fuyuki, *Sol. Energ. Mat. Sol. C.* **90** No 16, 2647 (2006).
2. J. Greulich, A.K. Volk, N. Wohrle, I. Haedrich, M. Wiese, M. Hermle, S. Rein, *Energy Procedia* **77**, 69 (2015).
3. V.F. Onyshchenko, *J. Nano - and Electron. Phys.* **15** No 3, 03026 (2023).
4. S. Manzoor, M. Filipic, A. Onno, M. Topic, Z.C. Holman, *J. Appl. Phys.* **127** No 6, 063104 (2020).
5. A. Alasfour, Z.J. Yu, W. Weigand, D. Quispe, Z.C. Holma, *Sol. Energ. Mat. Sol. C.* **218**, 110761 (2020).
6. C.S. Schuster, A. Bozzola, L.C. Andreani, T.F. Krauss, *Opt. Express* **22**, A542 (2014).
7. M. Otto, M. Kroll, T. Kasebier, R. Salzer, A. Tunnermann, R.B. Wehrspohn, *Appl. Phys. Lett.* **100**, 191603 (2012).
8. V.F. Onyshchenko L.A. Karachevtseva, K.V. Andrieieva, N.V. Dmytruk, A.Z. Evmenova, *Semiconductor Physics, Quantum Electronics & Optoelectronics* **26** No 2, 159 (2023).
9. V.F. Onyshchenko, *J. Nano- Electron. Phys.* **14** No 5, 05024 (2022).
10. O. Hohn, N. Tucher, B. Blasi, *Opt. Express* **26** No 6, A320 (2018).
11. S.C. Baker-Finch, K.R. McIntosh, *Prog. Photovoltaics Res. Appl.* **21** No 5, 960 (2013).
12. V.F. Onyshchenko, *Ukr. J. Phys.* **67** No 12, 841 (2022).
13. A.A. Fashina, K.K. Adama, O.K. Oyewole, V.C. Anye, J. Asare, M.G. Zebaze Kana, W.O. Soboyejo, *Journal of Renewable and Sustainable Energy* **7**, 063119 (2015).
14. P. Dhawan, M. Gaudig, A. Sprafke, R. Wehrspohn, C. Rockstuhl, *Opt. Express* **29** No 13 19903 (2021).
15. V.F. Onyshchenko, L.A. Karachevtseva, *J. Nano- Electron. Phys.* **17** No 1, 01022 (2025).

Відбиття двостороннього пористого кремнію з макропорами або нанодротинами

В.Ф. Онищенко, Л.А. Карачевцева

Інститут фізики напівпровідників імені В.Є. Лашкарьова НАН України, 03028 Київ, Україна

Відбиття двостороннього пористого кремнію з макропорами або нанодротинами розраховано за аналітично виведеними формулами. Формули враховують багаторазове відбиття світла під всіма кутами в кожному пористому шарі та монокристалічній підкладці. Шари пористого кремнію розглядаються як ефективні середовища з Ламбертовими поверхнями. Відбиття двостороннього макропористого кремнію залежить від об'ємної частки пор фронтального пористого шару. Товщина фронтального шару макропористого кремнію впливає на спектр відбиття двостороннього макропористого кремнію, коли об'ємна частка пор більше 0,2. Влив товщини фронтального шару макропористого кремнію на спектра відбиття двостороннього макропористого кремнію зростає, коли об'ємна частка пор зростає. Об'ємна частка пор тильного шару макропористого кремнію впливає на спектр відбиття двостороннього макропористого кремнію при довжинах хвиль світла більших за 1,05 мкм.

Ключові слова: Відбиття, Двошаровий пористий кремній, Макропористий кремній, Нанодротини.